Thermoelectric power factor in semiconductors with buried epitaxial semimetallic nanoparticles

J. M. Zide, D. O. Klenov, S. Stemmer, and A. C. Gossard
Department of Materials, University of California, Santa Barbara, California 93106-5050

G. Zeng and J. E. Bowers
Department of Electrical and Computer Engineering, University of California, Santa Barbara, CA 93106

D. Vashaee and A. Shakouri
Jack Baskin School of Engineering, University of California, Santa Cruz, California 95064

(Received 9 May 2005; accepted 21 July 2005; published online 7 September 2005)

We have grown composite epitaxial materials that consist of semimetallic ErAs nanoparticles embedded in a semiconducting $In_{0.53}Ga_{0.47}As$ matrix both as superlattices and randomly distributed throughout the matrix. The presence of these particles increases the free electron concentration in the material while providing scattering centers for phonons. We measure electron concentration, mobility, and Seebeck coefficient of these materials and discuss their potential for use in thermoelectric power generators. © *2005 American Institute of Physics*. [DOI: 10.1063/1.2043241]

Much of the recent work on thermoelectric materials has focused on the ability of heterostructures and quantum confinement to increase efficiency over bulk materials.[1–6] Optimal materials have high electrical conductivity, low thermal conductivity, and a high Seebeck coefficient, which results in a large figure of merit, $ZT=S^2\sigma T/\kappa$, where S is the Seebeck coefficient, σ is electrical conductivity, and κ is thermal conductivity.

Incorporating semimetallic nanoparticles into a semiconductor can have a large effect on the properties of the semiconductor. The particles can act as dopants,[7] buried Schottky barriers,[8] deep states for carrier recombination[9] or enhanced tunneling,[10] and phonon scattering centers.[11,12] Unlike bulk thermoelectric materials, these composites have the advantage of compatibility with the complex structures traditionally associated with semiconductor thin films, which allows the consideration of increasing the Seebeck coefficient via electron filtering[13] as well as architectures which are optimized for the temperature gradient through the thickness of the device.

Recent work has demonstrated the growth of structures consisting of superlattices of self-assembled semimetallic ErAs particles in a matrix of GaAs or $In_{0.53}Ga_{0.47}As$. The nanometer sized particles grow epitaxially in the rocksalt crystal structure.[14] Incorporating ErAs into InGaAs produces n-type material with a free electron concentration which increases with decreasing particle size.[7] We studied two types of sample structures in detail, which will be referred to as structures A and B (Fig. 1). Structure A consists of a superlattice of ErAs islands in InGaAs with ErAs depositions of 0.05, 0.1, 0.2, and 0.4 monolayers (ML) per period and layer spacings of 5, 10, 20, and, 40 nm. Layer spacings were chosen to keep the total atomic fraction of ErAs fixed at 0.3%, and the number of periods were chosen to keep a constant total thickness of 1.2 μm. Particle depositions are stated as though the ErAs grew in a layer-by-layer growth mode; larger depositions result in larger islands.[15] For each structure, a sample was grown both doped solely by ErAs and co-doped with 5×10^{18} cm^{-3} silicon. Structure B contains ErAs particles randomly distributed throughout the semiconductor and has the same thickness of 1.2 μm and atomic fraction of 0.3%. Each sample is grown on a buffer layer of 100 nm InAlAs and 40 nm n-InGaAs, lattice-matched to an InP substrate. The ErAs has a lattice mismatch of ~2% to the substrate and films.

All samples were grown using a Varian Gen II molecular beam epitaxy system on (100) semi-insulating InP:Fe substrates. The substrate temperature was measured at 490 °C using a pyrometer. Further details regarding the growth and structure of the Structure A particles have been discussed previously.[7,14,15] Structure B was grown by codepositing erbium at a growth rate corresponding to the desired atomic fraction during the growth of the semiconductor. Growth rates for ErAs were determined by beam fluxes from the erbium source. Cross-section transmission electron microscopy samples of this structure were prepared by standard TEM sample preparation techniques with 3 kV Ar ion milling as the final step (Gatan PIPS). High-resolution TEM (HRTEM) was performed using a field-emission TEM (Tecnai F30U) with ultratwin objective lens (Cs=0.52 mm), operated at 300 kV. A cross-section high-resolution transmission electron micrograph of the structure B sample is shown in Fig. 2.

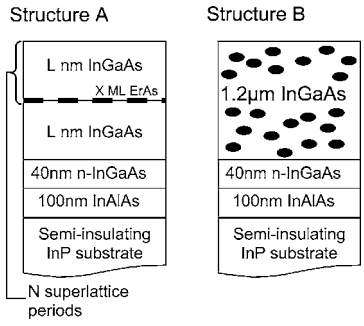

FIG. 1. Sample structures of ErAs:InGaAs materials. Structure A consists of superlattices of ErAs particles with depositions ranging from 0.05–0.4 ML and layer spacings ranging from 5 to 40 nm. Structure B consists of randomly distributed particles codeposited during semiconductor growth. Each sample is grown on a buffer layer of 100 nm InAlAs and 40 nm n-InGaAs (5×10^{18} cm^{-3} Si doped). All samples contain an average 0.3 at. % of ErAs.

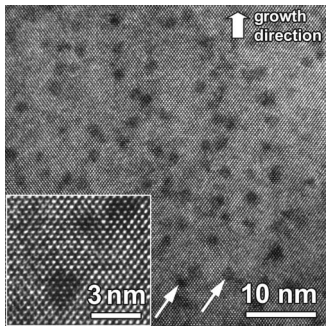

FIG. 2. High-resolution cross-sectional transmission electron micrograph of randomly distributed particles (structure B). The micrograph confirms the formation of nanometer sized particles. The spatial distribution of the particles appears to be essentially random. For clarity, several particles are highlighted with arrows.

The electrical conductivity of each sample was measured using room temperature Hall measurements in a van der Pauw geometry. The free electron concentration and mobility of each sample are plotted in Figs. 3(a) and 3(b), respectively. The free electron concentration decreases with increasing particle size, which is in agreement with earlier work. In addition, temperature-dependent Hall measurements were taken of structure B and the structure A sample containing the smallest particles. The obtained free electron concentrations and mobilities as a function of temperature from 4–400 K are plotted in Fig. 4. Structure B is similar in electrical conductivity to structure A.

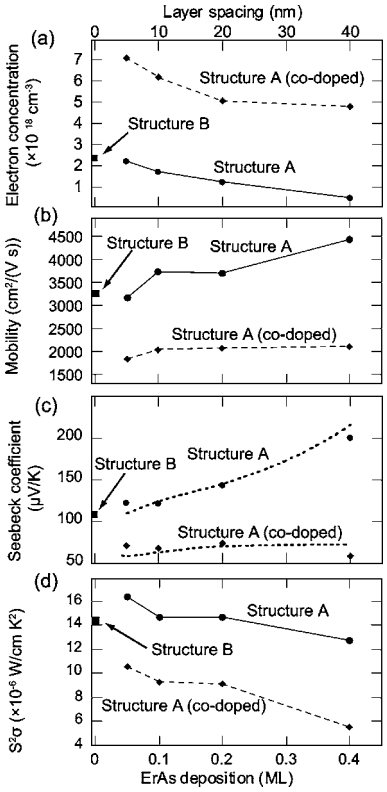

FIG. 3. Electronic properties of ErAs:InGaAs structures (a) free electron concentration vs ML of ErAs deposition of structure A with ErAs only (circles, solid line), structure A with 5×10^{18} cm^{-3} Si codoping (diamonds, dashed line) and structure B (square) at room temperature; (b) electron mobility of structures A and B at room temperature; (c) in-plane Seebeck coefficient of structures A and B. The dotted curves are calculated using a linear Boltzmann transport equation; (d) $S^2\sigma$, which appears in the thermoelectric figure of merit, of structures A and B.

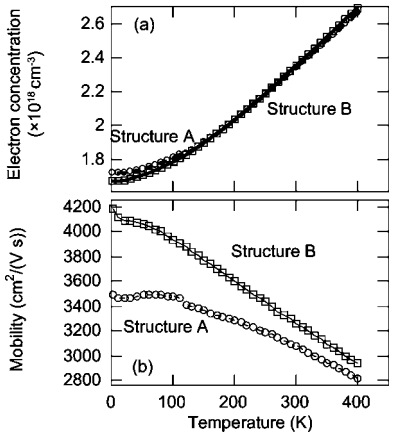

FIG. 4. Temperature dependent Hall data comparing the structure A sample with 0.05 ML deposition and 5 nm spacing (circles) with structure B (squares) over the temperature range 4–400 K; (a) free electron concentration; (b) electron mobility.

The Seebeck coefficient is the ratio of the voltage across a thermal gradient to the magnitude of that gradient and was measured by using a thermoelectric cooler to create a gradient across a small sample of each structure. Metal contacts were patterned and the differences in voltage and temperature across the gradient were measured. To calculate the theoretical Seebeck coefficient of the materials, we used the model presented in Ref. 16. In brief, a linear Boltzmann transport equation was used to calculate the thermoelectric characteristics of the materials. Free electron density data from the Hall measurement [Fig. 3(a)] was used to estimate the Fermi energy. The theoretical in-plane Seebeck coefficients of the materials were then calculated assuming an effective electron mass of $0.06m_e$ and a nonparabolicity coefficient of 1.167 eV^{-1}.[17] A momentum relaxation time of 0.063 to 0.15 ps was assumed which matches the experimental mobility data in Fig. 3(b) (1851 cm^2/Vs for a doping of 7×10^{18}cm^{-3} and 4430 cm^2/V s for a doping of 4.5×10^{17}cm^{-3}). In Fig. 3(c), the theoretical Seebeck coefficient (dotted curve) and experimental values of Seebeck coefficient (points) are compared. As expected, the measured Seebeck coefficient decreases with increasing electron concentration and agrees reasonably well with the calculated values.

In Fig. 3(d), the thermoelectric power factor, $S^2\sigma$, is plotted. The figure of merit is higher for samples with smaller particles and without silicon codoping. Measurements of thermal conductivity (in the cross-plane direction) on these samples have been reported elsewhere[18,19] and show a decrease in thermal conductivity by approximately a factor of 2–3. The decreases are only relatively weakly dependent on particle size. Neglecting this weak dependence, the highest ZT would be obtained in the samples with the smallest depositions.

The measurements of electrical and thermoelectric properties were performed in the plane of the wafer, while power generators could use either in-plane or cross-plane directions. Structure B should be isotropic, but the electrical properties of structure A may vary substantially in the cross-plane direction. The measured electron mobility in structure A is an average mobility. The actual mobility is likely to vary as a function of distance from the ErAs layers, with lower mobilities in layers containing ErAs and higher mobilities

between layers. Cross-plane electrical conductivity and Seebeck coefficients are difficult to measure directly. Besides the advantage of unambiguous measurement of electrical properties due to isotropy, structure B has the additional advantage of not requiring growth interrupts. This results in a faster growth and therefore less concern about the stability of sources in a relatively long molecular beam epitaxy growth.

In summary, ErAs increases the free electron concentration of InGaAs while maintaining relatively high mobilities. Seebeck coefficients in reasonable agreement with a linear Boltzmann transport model were measured for several sample structures. One of the key advantages of the ErAs:InGaAs system for thermoelectric materials is the relative ease in which techniques like electron filtering[13] can be used to increase the Seebeck coefficient while maintaining higher electron concentrations. Planar barriers of $In_{0.52}Al_{0.48}As$ or $In_{0.52}Ga_xAl_{0.48-x}As$ can be used to prevent the transmission of less energetic electrons. Measurements of the ErAs:GaAs system[20] suggest that the particles may function as nonplanar barriers in order to break the conservation of lateral momentum, which has the potential to greatly increase the efficiency of these materials. Taken together with the encouraging results of thermal conductivity measurements, this work suggests that embedded metallic nanoparticles in a semiconductor matrix can serve as a building block for creating efficient thermoelectric materials.

This work was supported by the Office of Naval Research as part of a MURI monitored by Dr. Mihal E. Gross.

[1] T. C. Harman, P. J. Taylor, M. P. Walsh, and B. E. LaForge, Science **297**, 5590, 2229 (2002).
[2] L. D. Hicks and M. S. Dresselhaus, Phys. Rev. B **47**, 16631 (1993).
[3] L. D. Hicks and M. S. Dresselhaus, Phys. Rev. B **47**, 12727 (1993).
[4] L. D. Hicks, T. C. Harman, and M. S. Dresselhaus, Appl. Phys. Lett. **63**, 3230 (1993).
[5] T. E. Humphrey and H. Linke, Phys. Rev. Lett. **94**, 096601/1 (2005).
[6] R. Venkatasubramanian, E. Siivola, T. Colpitts, and B. O'Quinn, Nature (London) **413**, 597 (2001).
[7] D. C. Driscoll, M. Hanson, C. Kadow, and A. C. Gossard, Appl. Phys. Lett. **78**, 1703 (2001).
[8] A. Dorn, M. Peter, S. Kicin, T. Ihn, K. Ensslin, D. Driscoll, and A. C. Gossard, Appl. Phys. Lett. **82**, 2631 (2003).
[9] C. Kadow, S. B. Fleischer, J. P. Ibbetson, J. E. Bowers, and A. C. Gossard, Appl. Phys. Lett. **75**, 3548 (1999).
[10] P. Pohl, F. H. Renner, M. Eckardt, A. Schwanhausser, A. Friedrich, O. Yuksekdag, S. Malzer, G. H. Dohler, P. Kiesel, D. Driscoll M. Hanson, and A. C. GossardAppl. Phys. Lett. **83**, 4035 (2003).
[11] D. G. Cahill, K. Goodson, and A. Majumdar, J. Heat Transfer **124**, 223 (2002).
[12] D. G. Cahill, W. K. Ford, K. E. Goodson, G. D. Mahan, A. Majumdar, H. J. Maris, R. Merlin, and S. R. Phillpot, J. Appl. Phys. **93**, 793 (2003).
[13] D. Vashaee and A. Shakouri, Phys. Rev. Lett. **92**, 106103/1 (2004).
[14] D. O. Klenov, D. C. Driscoll, A. C. Gossard, and S. Stemmer, Appl. Phys. Lett. **86**, 111912 (2005).
[15] D. C. Driscoll, M. P. Hanson, E. Mueller, and A. C. Gossard, J. Cryst. Growth **251**, 243 (2003).
[16] D. Vashaee and A. Shakouri, J. Appl. Phys. **95**, 1233 (2004).
[17] *Landolt-Börnstein* (Springer, Heidelberg, 2001), Vol. 41/Group III-Condensed Matter.
[18] W. Kim, P. Reddy, A. Majumdar, J. Zide, A. Gossard, G. Zeng, J. Bowers, and A. Shakouri, presented at the ASME Integrated Nanosystems, Pasadena, CA, 2004.
[19] W. Kim, J. M. Zide, A. C. Gossard, D. O. Klenov, S. Stemmer, A. Shakouri, and A. Majumdar, Nat. Mater. (2005).
[20] K. J. Russell, Ian Appelbaum, V. Narayanamurti, M. P. Hanson, and A. C. Gossard, Phys. Rev. B **71**, 121311(R) (2005).